SAND80-0012
Unlimited Release
UC-62

Performance Testing of the Scientific Atlanta Faceted Fixed Mirror Solar Concentrator

Vernon E. Dudley, EG&G Inc.
Robert M. Workhoven

Prepared by Sandia Laboratories, Albuquerque, New Mexico 87185
and Livermore, California 94550 for the United States Department
of Energy under Contract DE-AC04-76DP00789

Printed January 1980

When printing a copy of any digitized SAND Report, you are required to update the markings to current standards.

Sandia Laboratories

2900 Q(7-73)

Issued by Sandia Laboratories, operated for the United States Department of Energy by Sandia Corporation.

NOTICE

This report was prepared as an account of work sponsored by the United States Government. Neither the United States nor the Department of Energy, nor any of their employees, nor any of their contractors, subcontractors, or their employees, makes any warranty, express or implied, or assumes any legal liability or responsibility for the accuracy, completeness or usefulness of any information, apparatus, product or process disclosed, or represents that its use would not infringe privately owned rights.

Printed in the United States of America

Available from
National Technical Information Service
U. S. Department of Commerce
5285 Port Royal Road
Springfield, VA 22161

Price: Printed Copy **$4.50** ; Microfiche $3.00

SAND80-0012
Unlimited Release
Printed January 1980

PERFORMANCE TESTING OF THE SCIENTIFIC ATLANTA FACETED FIXED MIRROR SOLAR CONCENTRATOR

Vernon E. Dudley
Energy Measurements Group
EG&G

Robert M. Workhoven
Experimental Systems Operations Division 4721
Sandia Laboratories
Albuquerque, NM 87185

ABSTRACT

This report summarizes the efficiency and thermal loss tests performed on the Scientific Atlanta Faceted Fixed Mirror Solar Concentrator. Tests occurred during March and April 1978, at the Mid-temperature Solar Systems Test Facility, Sandia Laboratories, Albuquerque, New Mexico. Test temperatures ranged from 100°C to 300°C.

CONTENTS

ILLUSTRATIONS

TABLES

PERFORMANCE TESTING OF THE FACETED FIXED MIRROR SOLAR CONCENTRATOR

Introduction

A series of concentrating solar collector designs are being tested at the Collector Module Test Facility (CMTF), located at the Sandia Laboratories in Albuquerque, New Mexico. The CMTF is a part of the Mid-temperature Solar Systems Test Facility (MSSTF) at Sandia Laboratories. These facilities operate as part of a Department of Energy program to characterize selected collector modules for possible use in future energy systems. The Program Plan is contained in Reference 1. Several of the collector designs tested have been chosen to provide the energy input for solar powered demonstration projects.

Test Objective

The objective of this test series was performance characterization of the Faceted Fixed Mirror Solar Concentrator with primary emphasis on peak thermal efficiency at solar noon and the thermal losses of the receiver for fluid temperatures from 100 to 300°C.

Collector Description

Figure 1 is a photograph of the FFMC installed at the CMTF. The collector was constructed in place by Scientific Atlanta personnel. Assembly began January 13, 1978, and was accomplished by riveting together pre-formed sheet metal parts. Each mirror is a fixed facet; the collector assembly contains 28 rows of 12 mirrors each for a total of 336 mirrors. Each mirror is silvered, second surface glass, 7.34 cm wide, 75.6 cm long, and 0.246 cm thick. The total collector aperture area is 18.75 m^2. Concentration ratio of the FFMC, defined as the ratio of collector aperture area to receiver aperture area, is 20 to 1.

The array of flat reflecting facets produces a narrow focal line that follows a circular path as the sun moves (see Figure 2 for geometry of the light path). Because the focal line path is on the same basic cylinder as the mirror facets, the focal line can be tracked by a movable heat-receiver assembly that rotates about the center of curvature of the reflector module. The ideal minimum image width at the focus is equal to a single mirror facet width, plus an increment caused by the subtended angle of the sun. One of the mirror facets near the center of the module is tangent to the basic cylindrical curvature of the module. The remaining mirror facets are set at different angles such that all reflect incident light to the focus point. Using the tangent facet as a reference point, the surface angle of any other individual facet is one-fourth of the included angle between that facet and the tangent reference facet (see Figure 2). See Reference 2 for a more complete description of the optical principles of the FFMC.

The mirrors are clipped on the open side of U-shaped sheet metal supports; these supports are pop-riveted to seven sheet metal bulkheads that have a circular-faceted top edge. The support bulkheads are visible in Figure 1. Figure 3 is a sketch of the mirror support construction.

The receiver is a sheet metal assembly that faces the reflecting surface, and is attached to the collector assembly with a Y-shaped framework. The open face of the receiver has a low-iron glass window that covers seven parallel absorber tubes which are plated with a black chrome selective surface. A secondary reflector is

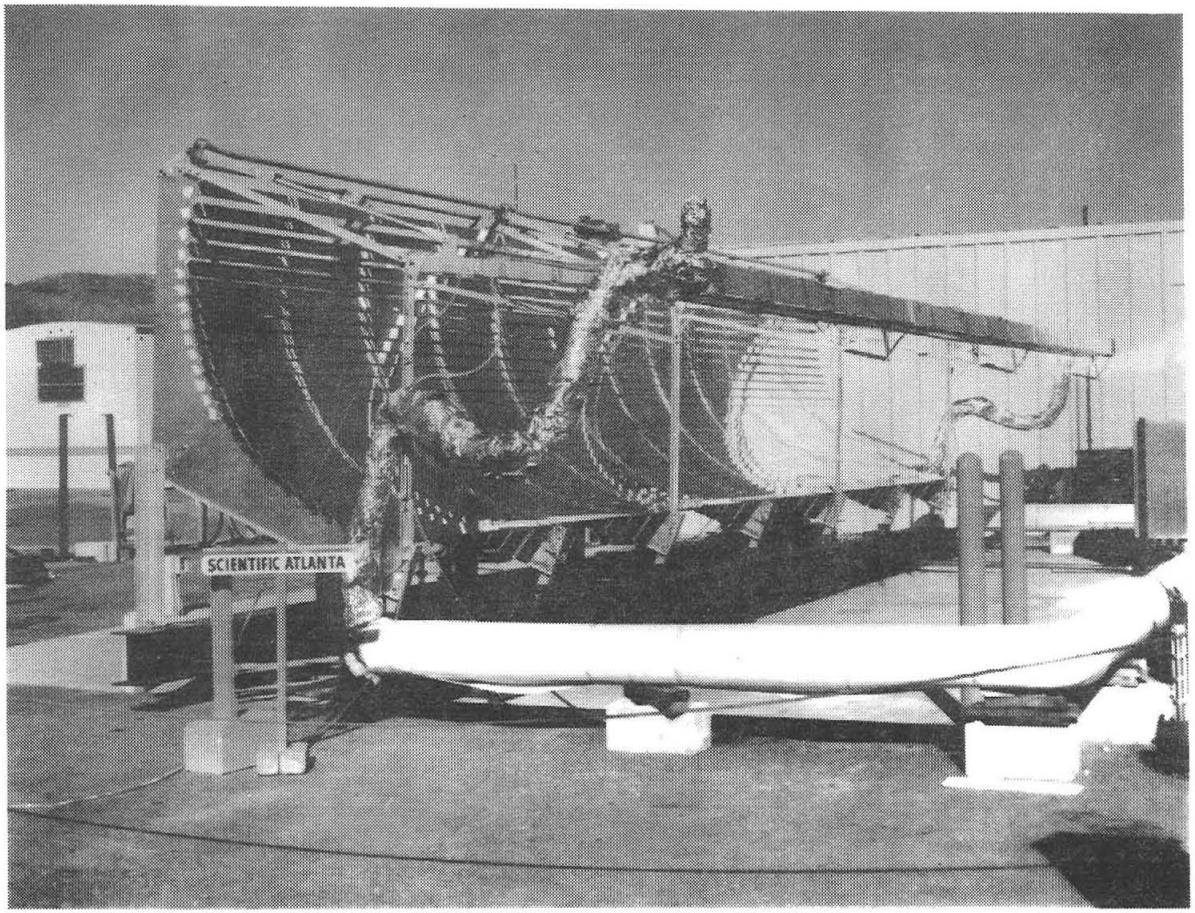

Figure 1. Scientific-Atlanta Collector.

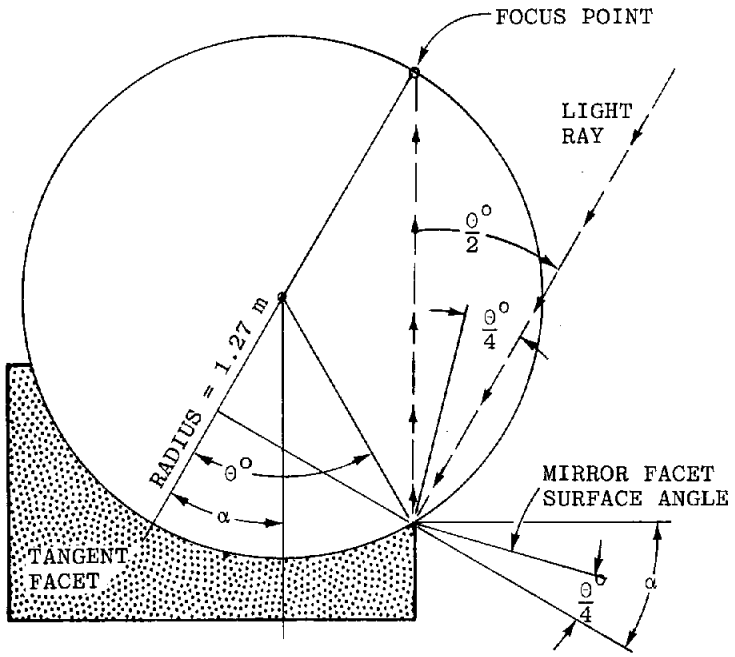

Figure 2. FFMC Light Path Geometry.

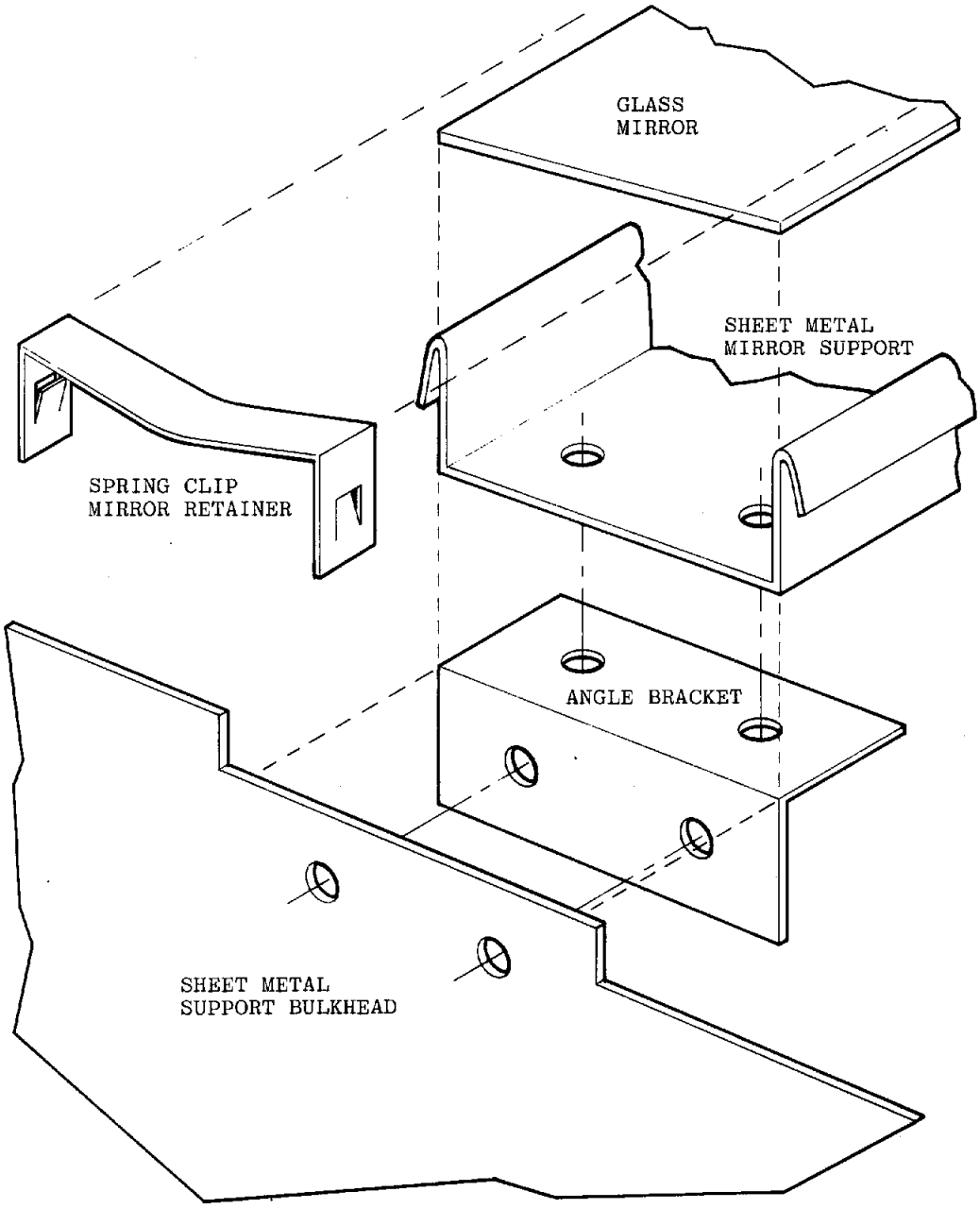

Figure 3. FFMC Mirror Support Construction.

fitted to the receiver to re-direct improperly focused sunlight. This secondary reflector is covered with FEK-244 film manufactured by the 3M company. The receiver is insulated on both sides and in back with the highly effective Microtherm^{R} insulation. See Figure 4 for a sketch showing a cross-section of the receiver. The receiver tracks the sun by using a photocell centered in the receiver aperture to provide analog signals to a mechanical drive system. Automatic control systems are provided to bring the receiver from a stowed position into focus when the light intensity is above a preset threshold. A return to the receiver stow position occurs when light intensity falls below the threshold.

Test Facility Description

The fluid loop used for this test series furnished a heat-transfer fluid to the collector module at input temperatures from 100 to 300^{o}C at flow-rates ranging from 4 to 40 liters/minute. The fluid used was Therminol-66, manufactured by the Monsanto Company.[3] Other general features of the Therminol fluid test loop used for this test are described in Reference 4.

The test on each day began by heating the fluid loop with electric heaters to the desired collector input temperature. Usually only one temperature point was attempted in one day due to the time required for temperature stabilization and the need to conduct efficiency tests near solar noon to minimize end effects. The collector system was placed in focus as early as possible each day so that recovered solar heat could aid in reaching the desired temperature. Temperatures near 200^{o}C could be attained by about 10:00 a.m. without difficulty while higher temperatures required much more time due to increasing thermal losses. The electric heaters were not large enough to heat the system to temperatures over 250^{o}C before noon without help from the collector system. For each test, input temperature and flow-rate were maintained constant while the output temperature varied according to test conditions.

The flow-rate of the Therminol-66 working fluid through the system was measured with a turbine flowmeter manufactured by Flow Technology, Inc. The flowmeter calibration was checked after the test series at three flow rates by flowing fluid into a tank and plotting tank weight vs time. A calibrated iron-constantan thermocouple was installed at each end of the receiver to determine temperatures into and out of the receiver. These two thermocouples were also connected as a differential pair for determining the delta temperature for calculations of heat gain or loss. A static mixer was incorporated at each end of the absorber tube to assure thorough mixing prior to measuring fluid temperature.

Differential pressure across the receiver was measured at several fluid temperatures and flow-rates as an indication of the pumping power required with a receiver of this design. Direct solar radiation was measured with an Eppley pyrheliometer. Ambient temperature, wind direction and wind speed measurements completed the active data collection.

Performance Test Definitions

During a test run, specific heat and density of the Therminol-66 fluid were calculated for each data set using the average temperature of the fluid in the absorber tube and fluid properties furnished by Monsanto Industrial Chemicals Company (Reference 3). Heat gain (or loss) was then calculated from the following

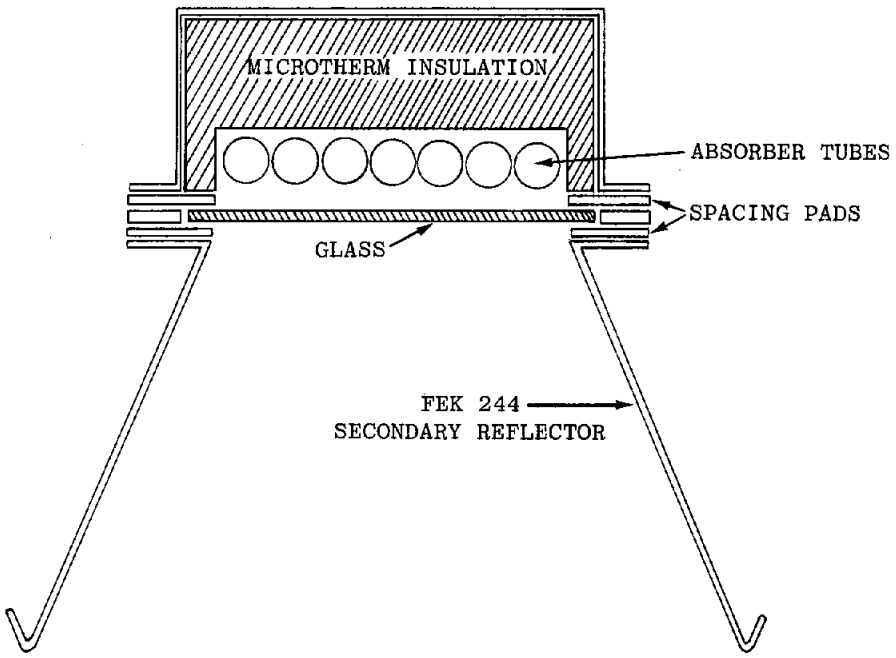

Figure 4. FFMC Receiver Cross Section.

formula:

$$Q = \dot{m} C_p \Delta T$$

in which

Q = heat gain, kJ/hr
$\dot{m}$ = mass flow-rate of fluid, kg/hr
C_p = specific heat of fluid, kJ/kg ^{o}C
ΔT = in/out temperature differential, ^{o}C

A successful thermal loss measurement was one in which the values for input temperatures remained constant for several minutes to within 0.1^{o}C or less, flow-rate varied by 0.1 liter/minute or less, and the temperature differential changed by 0.1^{o}C or less. Thermal loss tests were conducted with the collector system near its normal operating position, but sufficiently defocused so that no light from the mirror array would strike any part of the receiver assembly.

On most days, after reaching the desired temperature, loss measurements were made until about one hour before noon. Loss testing was resumed for about two hours after completion of solar noon efficiency tests; the fluid loop was then placed in a cooling mode prior to shutdown for the day.

For an efficiency test, efficiency was calculated from the following formula:

$$\eta = \frac{Q/A}{I}$$

in which

η = solar collector efficiency
Q = heat gain, W
A = collector aperture, m^2
I = solar radiation, W/m^2

An efficiency measurement at a single temperature and flow-rate was usually made from about one hour before noon until about one hour after noon to assure complete temperature and flow stabilization. This procedure provides good definition of the peak noon efficiency.

A successful efficiency data point measurement consists of at least one of the ten-point averages during which input and output temperatures changed by 0.1^{o}C or less, the delta temperature remained within 0.1^{o}C or less, and solar radiation remained constant to about 1%. Temperatures, flow-rate, and insolation had to have been nearly as stable as described above for at least five to ten minutes prior to the measurement, otherwise that data point was not considered to be a reliable measurement.

The temperature, flow-rate and insolation stability criteria outlined above are necessary because the heat gain formula given assumes steady state conditions. If near steady state conditions can be achieved during a collector test, the computed values for heat gain (or loss) and efficiency will be nearly constant also, with some scatter in the data due to noise. Because of the thermal mass of the collector system, any change in temperature, flow or insolation will result in measurements that do not correctly represent the performance of the collector.

Even on a sunny day that appears ideal for testing a solar collector, there are still variations in solar radiation. However these variations can be relatively small, as can be seen in several of the test data plots later in this report. Small, rapid variations of this kind produce scatter in the efficiency data, but no long term systematic errors.

As operated at the CMTF, the heat transfer fluid supply loop tends to produce fluid flow rate variations similar to those seen in the solar radiation input: small, rapid fluctuations with no long term trend towards a higher or lower rate. These variations also produce scatter in the measured data.

Small rapid temperature fluctuations also appear in the measured data, again producing data scatter. However, the temperature measurements are subject to fairly long term, slow changes which can result in fairly large, systematic errors in heat gain/loss and efficiency calculations. One typical source of this kind of temperature drift is the constantly increasing temperature that occurs each test day as the system is heated towards the intended operating temperature. Another is the temperature decay that continues for very long times after the collector system is defocused to begin a thermal loss test.

At the CMTF, collector input and output temperatures are usually measured less than one second apart in time. However, the fluid whose temperature is being measured at the collector input may not arrive at the collector output thermocouple for a relatively long time--from several seconds up to several minutes. Thus an efficiency or heat gain/loss measurement will not be valid unless the input and output temperatures are unchanging for at least as long as the transit time of the heat transfer fluid through the system.

Because of the thermal mass of both the fluid supply system and the collector, stable temperatures must be held for relatively long periods of time before the complete system is in thermal equilibrium and valid measurements can be made. A small constant drift in temperatures can produce test data that looks quite acceptable, but which contains a systematic error because of the thermal mass shift of in-out delta temperature. For example, on one collector tested, a constant temperature increase of $0.7^{\circ}C$ per minute produced an efficiency measurement that had a very small data scatter and had a nearly constant efficiency value for more than an hour. This measured efficiency value turned out to be 5 percentage points lower than the efficiency measured later with more stable temperatures. In another case, with a collector system of greater thermal mass, a similar slow drift in input temperature produced an efficiency measurement 15 percentage points lower than the true value.

If the input temperature drift is towards lower temperatures, errors of similar magnitude result, but the measured efficiency will now be greater than the value obtained under stable conditions.

The same problem as outlined above for an efficiency measurement also occurs during thermal loss measurements. Since the receiver delta temperature during a loss test is usually much less than during an efficiency measurement, the error in thermal loss from unstable temperatures is larger than the efficiency error.

The requirement for $0.1^{\circ}C$ stability in measured temperatures for a useable data point is empirically based. It appears to produce valid data, and is also about as good as the fluid loop and collector system can attain in the outdoor test environment.

The data provided by the instruments described above was converted to a digital format by an analog-to-digital data system. A minicomputer processed the data and provided a printed output of critical data for the test being performed. Figures 5 and 6 are copies of the data output from an efficiency test and from a loss test, respectively. Unless otherwise labeled, the temperatures cited in those figures are in degrees Celsius.

The speed of the data system was such that all the data channels could be read, calculations could be performed, and a line in the data table could be printed in about 25 seconds. The average values were automatically printed after ten data points were accumulated. The complete data printout as shown in Figures 5 and 6 was repeated at intervals of about 3-4 minutes throughout a test run. 41 measured and calculated data values from the data system were recorded on magnetic tape every 25 seconds. Only those shown in Figures 5 and 6 were printed in real time. The number of decimal places in the data printout should not be taken as indicating the accuracy of the data system, since the choice of the print format was dictated by peculiarities of the computer system. Either a loss or an efficiency data print was made continously when the system was operating; however, only those data blocks occurring under stable conditions are included in this report.

Test Results

Testing of the FFMC began on 11 March 1978. Twenty efficiency tests and 29 thermal loss tests were made, concluding on 12 April 1978.

Initial efficiency tests produced results which looked much too low-below 40% efficiency at low temperatures. The flowmeters had recently been checked for calibration, so attention was focused on the fluid thermocouples. The two thermocouples (previously individually calibrated) used for receiver input and output temperatures were placed together at the input end and checked for tracking over a fluid temperature range from 60°C to 220°C. No significant discrepancy was found, so efficiency and loss testing was resumed.

Efficiency test data obtained is contained in Table 1.

Table 1. FFMC Peak Noon Efficiency

Test Date	Solar Radiation (W/m^2)	Temp Out (°C)	Receiver Temp (°C)	Flow Rate L/Min	Efficiency %
3/16/78	1078	208.3	6.8	30.4	33.4
3/17/78	1051	258.7	6.0	30.7	32.1
3/17/78	1049	258.9	7.8	20.2	29.0
8/18/78	1057	161.4	7.3	30.1	35.1
3/21/78	905	87.3	6.8	30.5	36.9
3/24/78	1067	169.3	18.2	10.4	30.0
3/29/78	966	263.2	13.0	10.2	24.9
3/30/78	1002	163.5	8.7	20.5	29.9
3/30/78	1000	168.4	13.9	10.9	27.4
3/31/78	1029	169.6	17.2	10.6	30.0
3/31/78	1030	158.9	5.9	30.5	30.8
4/02/78	1005	249.3	6.6	20.6	24.8
4/04/78	924	287.7	2.7	40.0	21.6
4/05/78	1033	160.4	4.4	39.9	28.6
4/06/78	1038	208.1	4.9	31.1	25.8
4/06/78	1037	212.5	12.5	10.4	23.3
4/07/78	1049	259.4	12.5	9.5	20.4
4/11/78	1013	209.6	9.3	20.4	32.8
4/11/78	1008	207.4	5.9	30.3	32.3
4/12/78	877	206.9	7.8	20.9	32.7

```
          ♦♦♦♦ SCIENTIFIC ATLANTA COLLECTOR EFFICIENCY TEST ♦♦

JULIAN DAY  80    HOUR  12    MINUTE  4       (SOLAR TIME)

 17.78          (DEG C)     AMBIENT TEMPERATURE     (DEG F)      64
 104             WIND DIRECTION, DEGREES
 .8             (M/SEC)      WIND SPEED       (MPH)               1.8

SKIN TEMPS       98.5            107.33          109

 TEMP             TEMP          SOLAR      DELTA          FLOW      EFFICIENCY
   IN              OUT        WATTS/M^2    TEMP        LITERS/MIN    PERCENT
 80.56           87.67          964.7       7.11          30.42         34.9
 80.61           87.83          988.9       7.22          30.46         36.8
 80.56           87.67          924.4       7.11          30.49         36.5
 80.56           87.56          905.6       7      30.48          36.6
 80.56           87.28          849.3       6.72          30.51         37.5
 80.56           87.28          868.8       6.72          30.48         36.6
 80.5            86.94          810.6       6.44          30.51         37.7
 80.5            86.61          801.4       6.11          30.51         36.1
 80.5            86.78          970.3       6.28          30.53         30.7
 80.44           87.83          1022.6      7.39          30.51         34.3

                    10 POINT AVERAGES
 80.535          87.345         904.66       6.81          30.49         35.77

 36.93          AVG EFFICIENCY USING DIFF. T.C.
 22475.8     AVG HEAT GAIN (KJ/HR)
 66.355         AVG. RECVR TEMP MINUS AMB. TEMP
 6.48885E-02     (AVG TEMP-AMB T)/I
 36.04       EFFICIENCY CORRECTED TO SOLAR NOON
```

Figure 5. Typical Data Printout, FFMC Efficiency Test

```
          ♦♦♦♦♦ SCIENTIFIC ATLANTA THERMAL LOSS TEST ♦♦♦♦

 JULIAN DAY  79    HOUR  13    MINUTE  31      (SOLAR TIME)

  18.06         (DEG C)     AMBIENT TEMPERATURE     (DEG F)      64.5
  117            WIND DIRECTION, DEGREES
  7.1           (M/SEC)      WIND SPEED       (MPH)               15.8

 ABSORBER SKIN TEMPS            75.44           76.5            73.61

  TEMP             TEMP         FLOW        DELTA          WATTS
    IN              OUT      LITERS/MIN      TEMP         GAIN/LOSS
  78.33           78.22         38.09        -.11          -121
  78.39           78.22         38.09        -.17          -186.9
  78.39           78.17         38.06        -.22          -241.7
  78.39           78.22         38.09        -.17          -186.9
  78.39           78.22         38.07        -.17          -186.8
  78.39           78.22         38.09        -.17          -186.9
  78.33           78.22         38.07        -.11          -120.9
  78.39           78.22         38.09        -.17          -186.9
  78.33           78.22         38.08        -.11          -120.9
  78.33           78.22         38.09        -.11          -121

                    10 POINT AVERAGES
  78.366          78.215         38.082       -.151         -166.002

 AVERAGE SOLAR INSOLATION =  216.09     WATTS/M^2
  76.959          AVG LOSS USING DIFF. T.C. (WATTS)
 AVG LOSSES: (KJ/HR)= -597.56      (W/M)= -18.3225     (W/M^2)= -8.87712
  60.215         AVG. RECVR TEMP MINUS AMB. TEMP
```

Figure 6. Typical Data Printout, FFMC Thermal Loss Test.

The same data is plotted in Figure 7 as efficiency vs fluid output temperature. Figure 8 is also the same efficiency data points plotted as efficiency vs average receiver temperature above ambient temperature divided by input solar radiation.

The curve shown in Figure 7 is drawn through the data points obtained in the first four days of testing. Because these efficiencies were relatively low, the fluid temperature thermocouples were checked, as noted previously; the mirror system and receiver glass were carefully cleaned, and additional tests were made at flow-rates from 10 to 40 liters per minute. No improvement in efficiency resulted; in fact, the measured efficiencies appeared to decrease as testing proceeded.

Some of the light from the mirrors was observed falling outside the receiver aperture. Visual observations through shade 12 glasses (plus a welder's helmet!) confirmed this light spillage. Light from some mirror segmets was found well above the entire receiver assembly. Light from others was found below the receiver and the light from many mirror segments was only partially within the receiver aperture.

Further checks were made of the collector's focal pattern. Figure 9 is a photograph of a plywood sheet held at the focal point. Two lines corresponding to the receiver aperture width were ruled on the sheet and centered within the light pattern. The concentrated light pattern appears about twice the width of the available receiver aperture. Similar photographs were made over the complete receiver length with similar results.

To define more quantititatively the amount of lost light, intensity scans were made across the receiver aperture for each row of mirror segments. A typical pattern is shown in the lower right corner of Figure 9. The intensity scan confirms the visual pattern also shown in Figure 9: much high intensity light was falling outside the receiver aperture. The light intensity scan curves have not been integrated to determine the exact percentage of the lost light.

In a further effort to understand the problems with the reflected light from the mirrors, photographs were again made of the light patterns on the plywood sheets. This time the patterns were observed at a position well beyond the focal point. For a perfect set of mirrors, all positioned at the correct angle, the pattern should appear as straight, parallel rows of light similar to the slats in a Venetian blind. A sample photograph is shown in Figure 10. The pattern obtained at other positions along the collector are similar.

The FFMC was installed on a structural steel support with the concentrator base tilted up at an angle of 22 degrees. This tilt is visible in Figure 1. This was done so that the solar radiation input would be normal to the center (tangent) mirror segment, thus simulating the light path geometry at the spring or fall equinox. The 22 degree tilt angle was chosen for a mid-winter test period. During the actual test period in March and April, the solar radiation was no longer normal to the tangent slat, but actually more closely simulated summer solistice conditions. In this position, solar radiation entered the mirror array from a high angle near the top, so that at solar noon, a number of the top rows of mirrors cast shadows on their neighbors immediately below. The shadowed area changed each day during the test period as the sun moved towards high elevations. Measurements and calculations were made of the shadowed area, termed "edge loss". Corrections to the efficiency data were calculated, using equations supplied by Scientific Atlanta, to remove the effects of the changing edge loss, in an attempt to reduce the wide

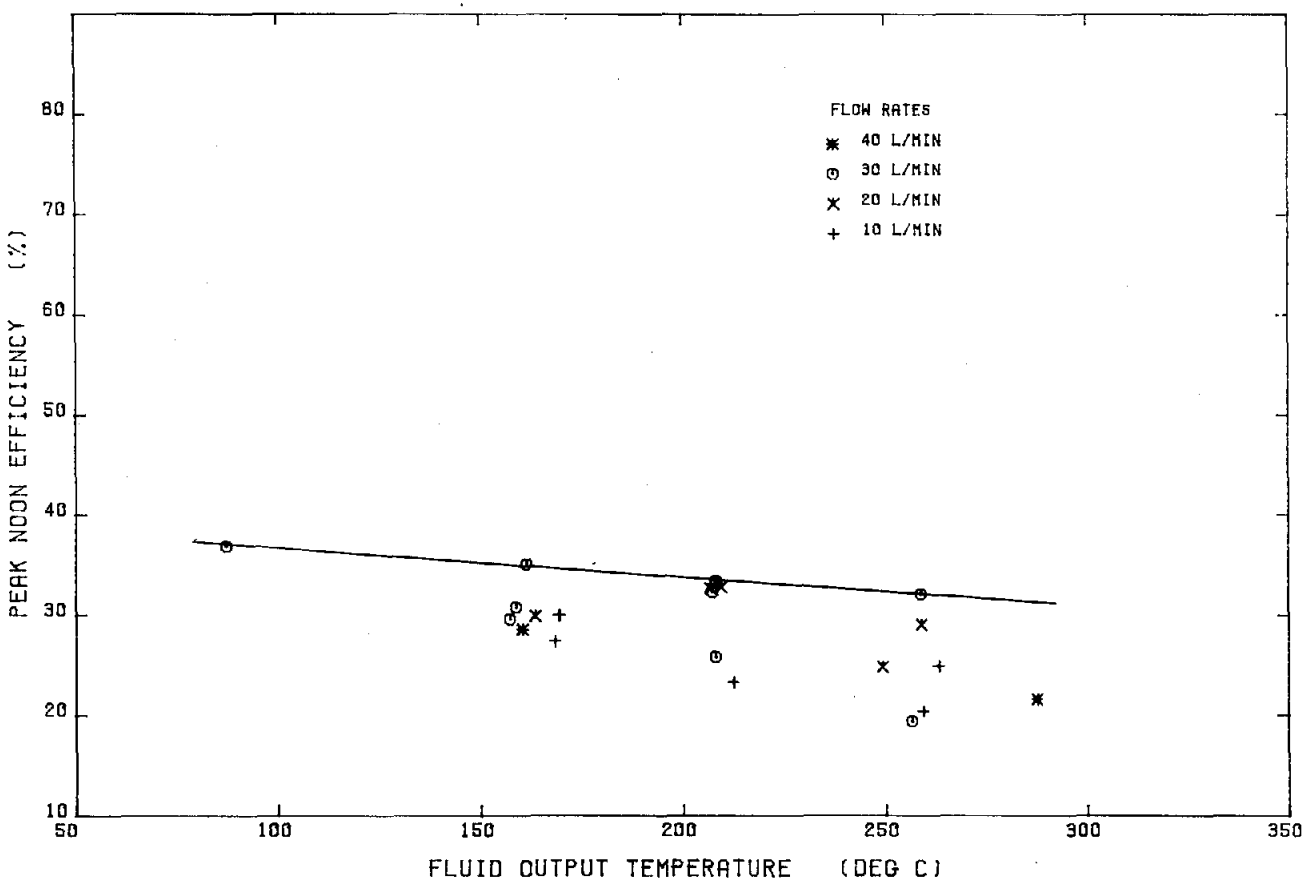

FIGURE 7 SCIENTIFIC ATLANTA FFMC EFFICIENCY (RAW DATA)

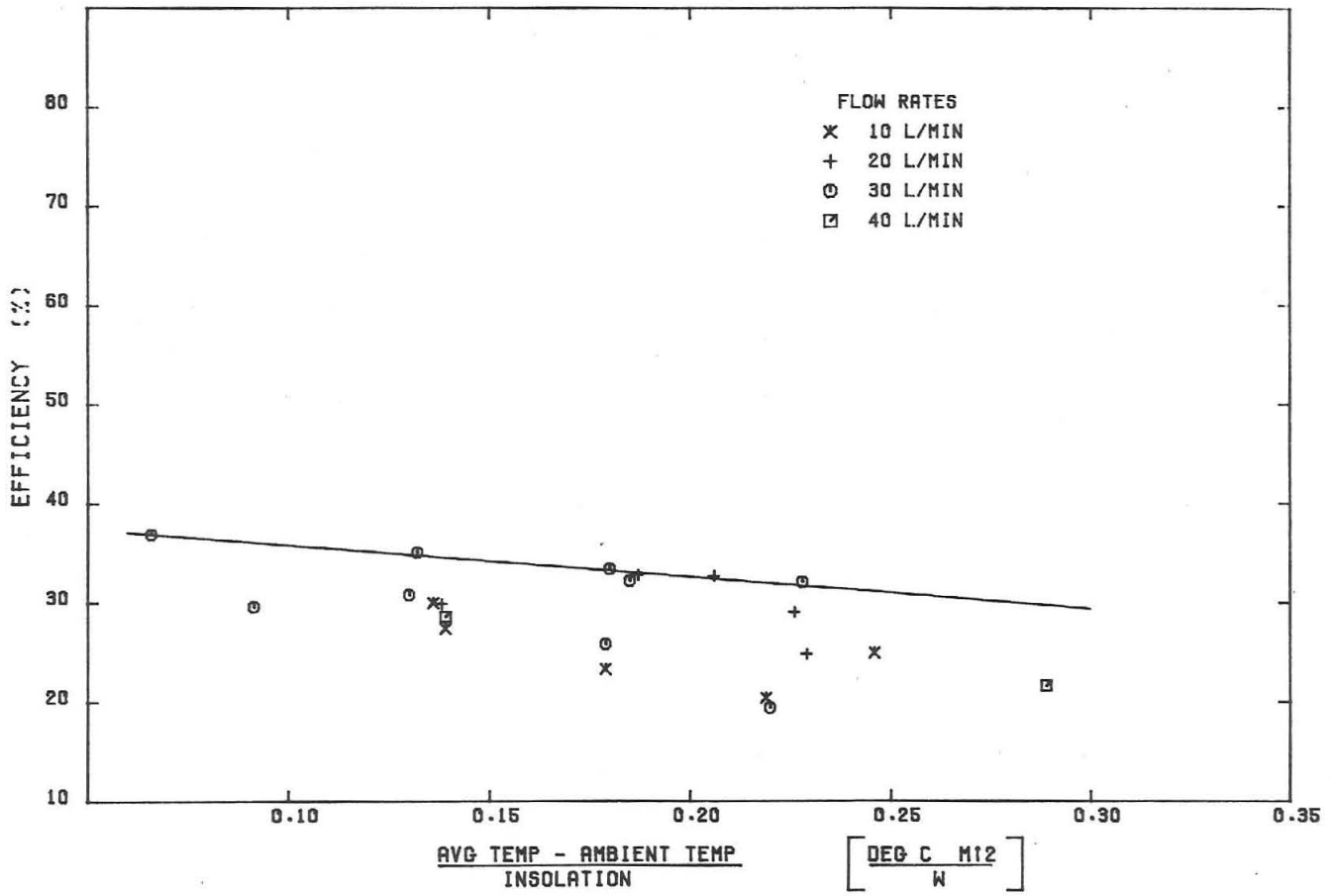

FIGURE 8 SCIENTIFIC ATLANTA FFMC EFFICIENCY VS DELTA TEMPERATURE / INSOLATION (RAW DATA)

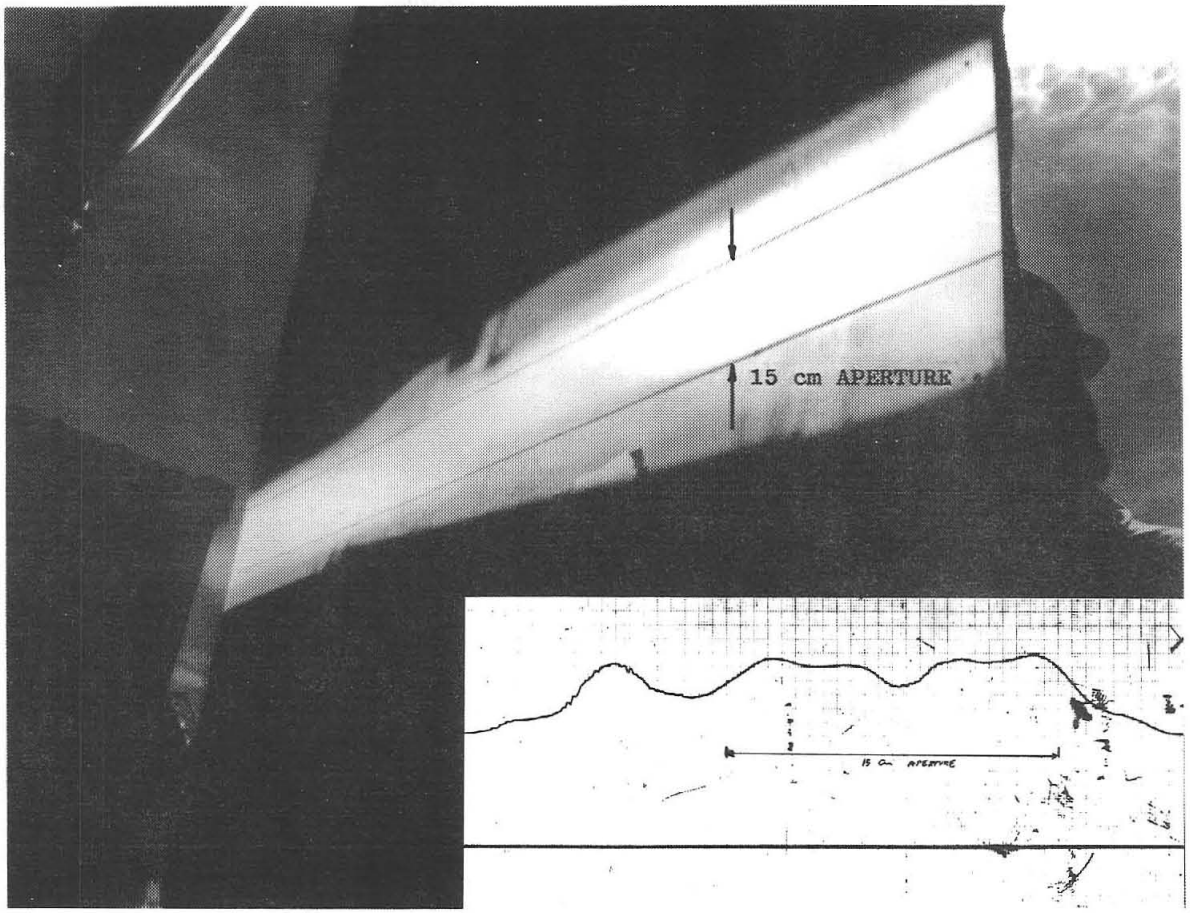

Figure 9. Light Pattern of the FFMC Collector at the Focal Point.

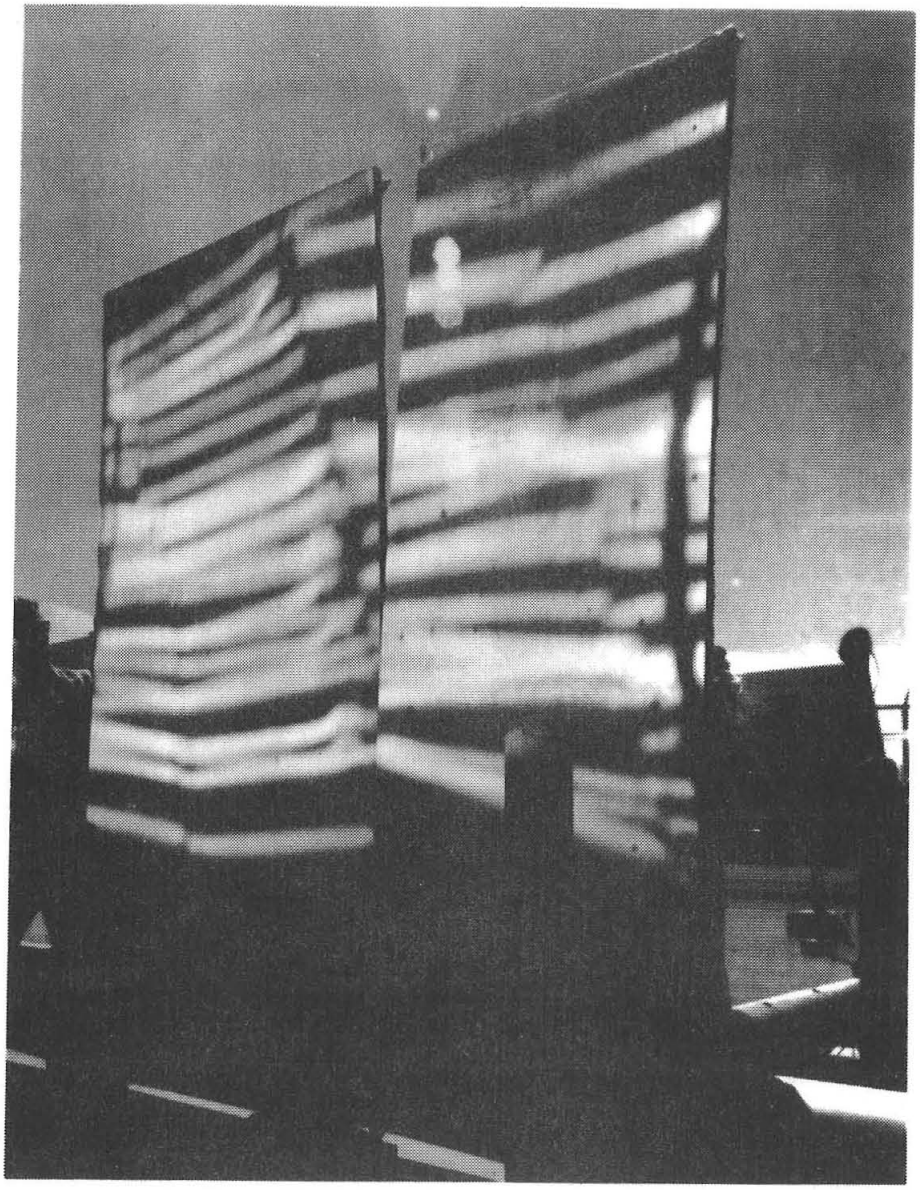

Figure 10. Light Pattern of the FFMC Collector Beyond the Focal Point.

scatter seen in the measured efficiency data. The resulting efficiency points are plotted in Figure 11. No notable change in data scatter is evident.

Figure 7 thus represents the efficiency attainable near summer solistice, while Figure 11 shows the approximate efficiencies that might be expected near the spring and fall equinoxes.

One final step was taken before concluding the efficiency test series. As originally built, the FFMC collector was not intended to be moved from its installed position, with a 22 degree base tilt angle. On April 10, structural steel supports and braces were added to the structure, and the collector was lowered to the horizontal base position that would normally be used in an operational installation.

Three additional efficiency tests were made (last three points in Table 1), in this new operating position. Much of the edge loss shadow was gone, but the shadow of the receiver assembly now fell on the mirror assembly. In the 22 degree tilted position, the receiver shadows fell off the forward edge of the mirror array; this receiver shadow position was just as abnormal as the relatively large mirror self-shadow (edge-loss) caused by the tilted collector. Since the area covered by the receiver shadow was about 60% as large as the edge loss shadow the measured efficiency was not very different from that measured before removing the tilt (about 33% at 207^{o}C).

Since the primary reason for the low measured efficiencies appeared to be lost light from mirrors that were not aimed at the receiver, some of the possible causes for inaccurate focus were investigated, and are discussed below.

Several conclusions can be drawn from Figure 10 and other similar photographs not shown in this report. (1) The light patterns from the individual mirrors are not parallel. This was confirmed by looking down the rows of mirrors from the ends of the collector; the larger out-of-parallel errors were easily seen. (2) The pattern variations appear more or less random from mirror to mirror, indicating errors in individual mirror placement, rather than some systematic error in building the array. Visual observation of the individual mirror aim point also indicates apparently random movement of mirrors from day to day. (3) The curves seen in a number of the light patterns occur at positions corresponding to the spring clips holding the glass to the underlying supports. Evidently, the downward force of the spring clip at the center of the unsupported glass bends the mirror slightly. (See Figures 3 and 4).

Assuming that all the assembly holes were properly located, one possibility for random mirror aim point variations may be the method used to rivet the mirror supports into position. A small amount of clearance is required to insert the rivets into the holes in the angle bracket and support bulkhead. (See Figure 3). Standard bucked rivets expand inside the rivet hole to fill the clearance space as they are compressed during installation. The pop-rivets used in this installation do not have this expansion characteristic during installation. Instead, pop-rivets expand <u>outside</u> the installation hole as the mandrel is pulled. This leaves any clearance between rivet and hole still available to appear as an angle error in the final mirror position. Because of the assembly geometry, any clearance in the rivet hole can be multiplied by up to a factor of 4 at the mirror surface. This factor alone would certainly not account for all the spilled light observed; however, a rivet hole clearance of only 0.010 cm (.004 inch) could result in loss of more than 20% of the light from the affected mirror. A deflection of only 0.34 cm

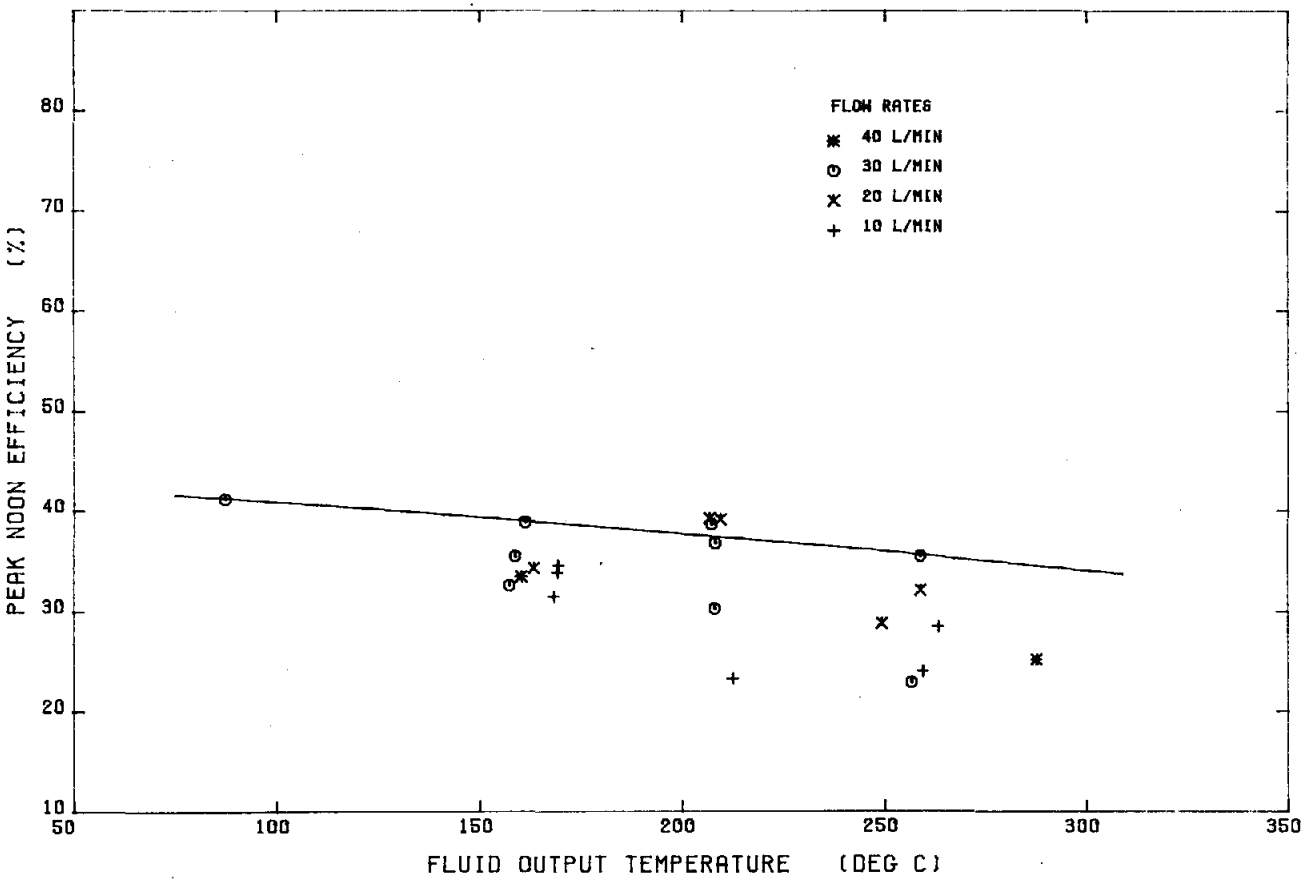

FIGURE 11 SCIENTIFIC ATLANTA FFMC EFFICIENCY (DATA CORRECTED FOR EDGE LOSS)

(0.134 inch) across the 7.34 cm wide mirrors is required for the reflected light to entirely miss the receiver.

Scatter in the test data indicates that changes in the structure occurred between test runs. Some changes may have been caused by wind stresses, thermal creep, etc. One certain factor was cleaning of the mirror surfaces. Because the retaining clips held the mirror segments fairly loosely, it was impossible to clean the mirror surfaces even with a soft brush without some mirror movement. Cleaning the mirrors only with a detergent spray and a deionized water rinse did not do a very good cleaning job. Even the relatively low pressure water spray also appeared to move some of the mirrors.

The problem with mirror movement is illustrated by Figure 12. The widths of mirror support channel, mirror and retaining clip were such that a movement fully to one side against the retaining clip allowed the opposite side of the mirror to begin to move down the inner curve at the top of the support channel, as illustrated in Figure 12. This mirror position resulted in shift in mirror aim point, with consequent loss of part or all of the reflected light. Measurements on only a few mirrors turned up one in which the dimension X in Figure 12 changed by 0.211 cm when the mirror was pushed to one side, fully against the retaining clip. As noted above, a deflection of about 0.34 cm would cause light from the mirror to entirely miss the receiver aperture.

Thermal loss data obtained from loss tests on the FFMC receiver is shown in Table 2, and in graphical form in Figure 13.

Table 2. FFMC Receiver Thermal Losses

Test Date	Average Temp Ambient Temp (°C)	Flow Rate L/Min	Solar Radiation (W/m^2)	Kj/hr	Loss Watts	W/m
3/11/78	141.2	14.8	57	2497	694	76.6
3/11/78	139.2	30.8	54	3205	891	98.3
3/11/78	136.8	5.4	1	2917	810	89.4
3/15/78	144.4	20.2	995	4206	1169	128.9
3/15/78	144.6	30.2	966	4609	1280	141.3
3/16/78	182.8	20.5	941	3592	988	110.1
3/17/78	224.3	10.2	958	4951	1375	151.8
3/17/78	228.9	20.4	926	4881	1356	149.7
3/18/78	139.9	21.9	1014	1897	527	58.2
3/18/78	138.4	40.1	1028	824	229	25.3
3/18/78	136.4	10.2	1047	2261	628	69.3
3/18/78	134.1	30.2	1034	1555	432	47.7
3/19/78	179.6	8.3	113	3951	1098	121.2
3/19/78	179.6	10.4	56	3354	932	102.8
3/19/78	181.7	20.1	266	3536	982	108.4
3/19/78	182.7	30.3	17	2874	798	88.1
3/19/78	182.5	40.0	59	2333	648	71.5
3/20/78	62.4	29.6	26	1126	313	34.5
3/20/78	60.2	38.1	216	597	166	18.3
3/20/78	63.9	20.4	48	1087	296	33.3
3/22/78	137.4	20.0	1	3088	858	94.7
3/24/78	133.2	10.4	1064	3050	847	93.5
3/24/78	134.0	20.4	1048	2846	791	87.3

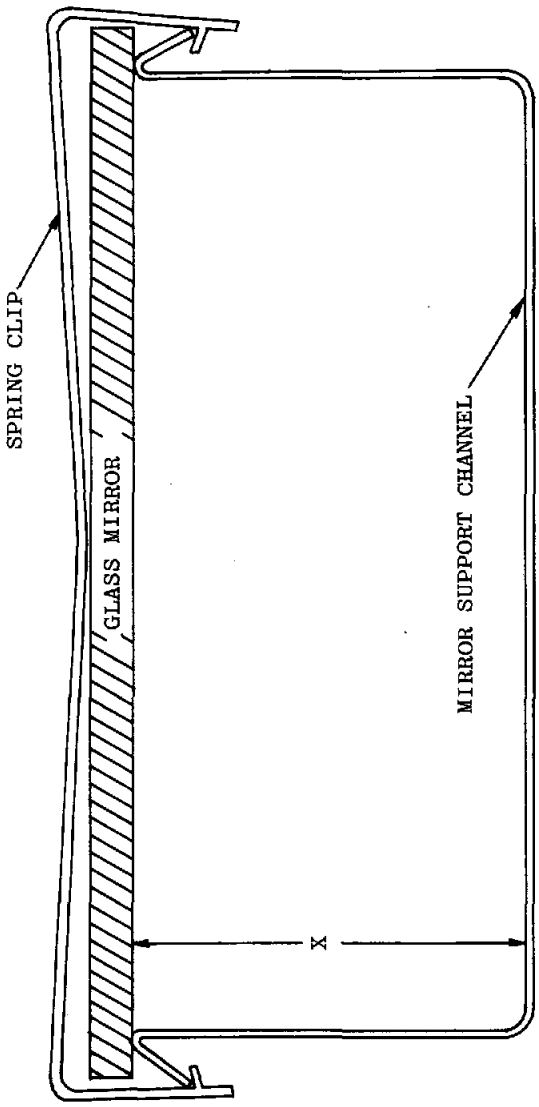

Figure 12. Sketch of Mirror Position.

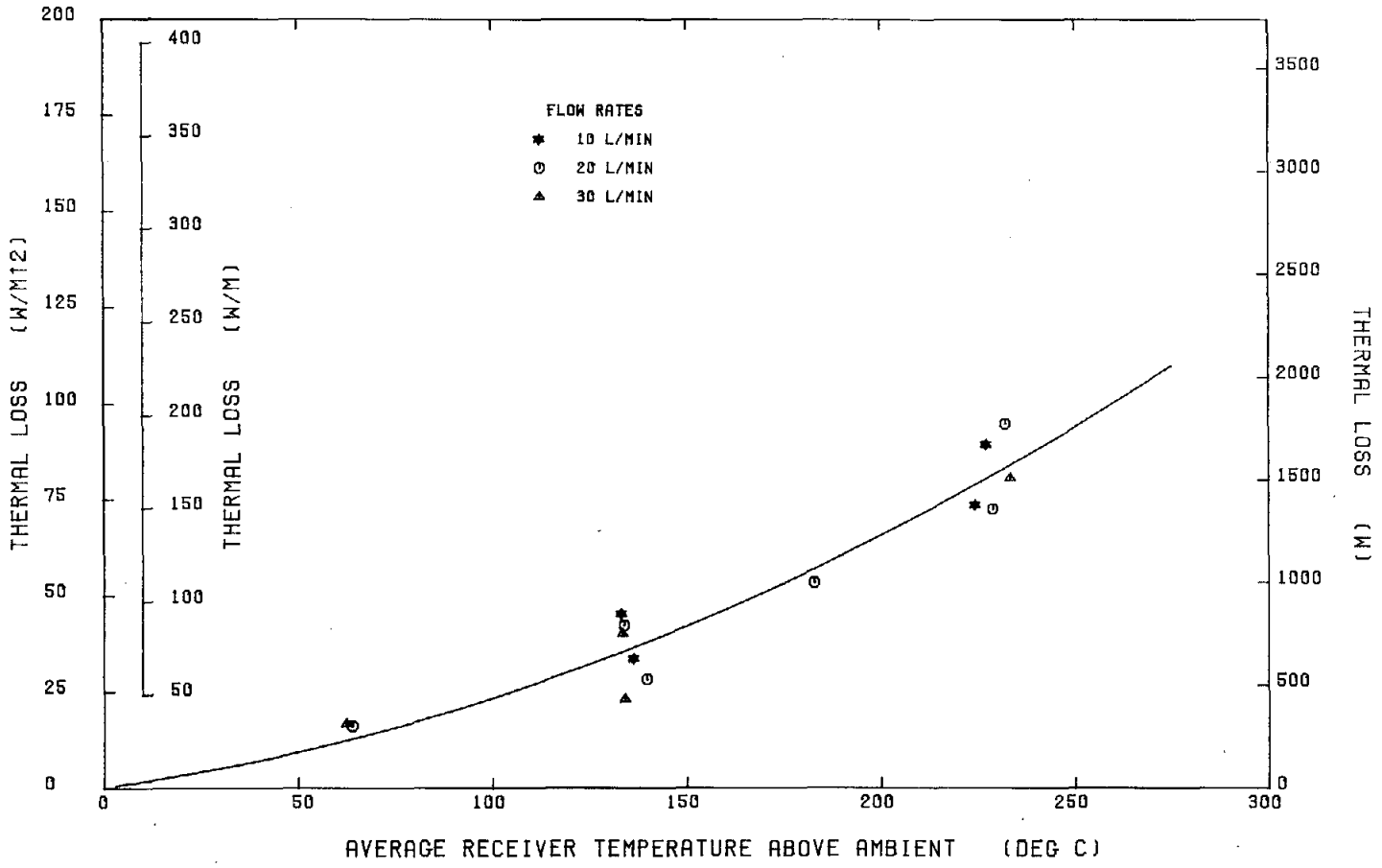

FIGURE 13 SCIENTIFIC ATLANTA RECEIVER THERMAL LOSS

Table 2 (Cont)

3/24/78	133.6	29.7	1039	2702	751	82.8
3/29/78	227.1	10.3	907	6020	1672	184.6
3/29/78	232.1	19.9	871	6391	1775	195.9
3/29/78	233.4	30.1	826	5429	1508	166.5
3/30/78	129.5	10.7	646	3774	1048	115.7
3/30/78	130.5	20.2	320	3140	872	96.3

The left ordinate in Figure 13 shows thermal loss as watts per square meter of collector aperture area and as watts per linear meter of receiver. The right ordinate shows the thermal loss in watts, as actually measured. Overall, the thermal loss data is more scattered than desirable, indicating that more time for temperature stabilization should have been allowed on several of the tests.

Shown below is the equation of the thermal loss curve, obtained from a least-squares fit to the data.

$$L = 0.250575 + 0.134697\ T + 9.60655E\text{-}04\ T^2$$

Where L = loss in watts/m^2

T = average receiver temperature above ambient (^{o}C)

The differential pressure across the receiver was measured at several temperatures, and at flow rates from about 4 to 40 liters/minute. The data was obtained with the receiver out of focus, in conjunction with thermal loss tests. Plots of some of this data is shown in Figure 14 for three fluid temperatures. The curves indicate the pumping power required for a receiver of this design.

On 9 August 1978, an unscheduled additional test was made on the FFMC, when a severe thunderstorm dumped large quantities of hail on the solar test area. Impact damage on soft aluminum and insulation in other parts of the test installation resulted in an estimate of 3/4 inch hailstones. Twenty eight mirrors were broken on the FFMC as a result of these 3/4 inch hailstones.

Summary of Results and Conclusions

The Scientific Atlanta FFMC did not perform as well as predicted by its designers. Maximum efficiency was just over 40% at low temperatures, and about 34% at 300^{o}C. Receiver thermal losses were relatively low, probably because of the very low conductivity of the Mircrotherm receiver insulation.

The problems found in this test series do not rule out the use of sheet metal in construction of a collector of this type. Sheet metal may have many advantages in weight, cost, simple production, ease of assembly, etc. The problems found with the test article can probably be corrected fairly easily in a redesign of the system.

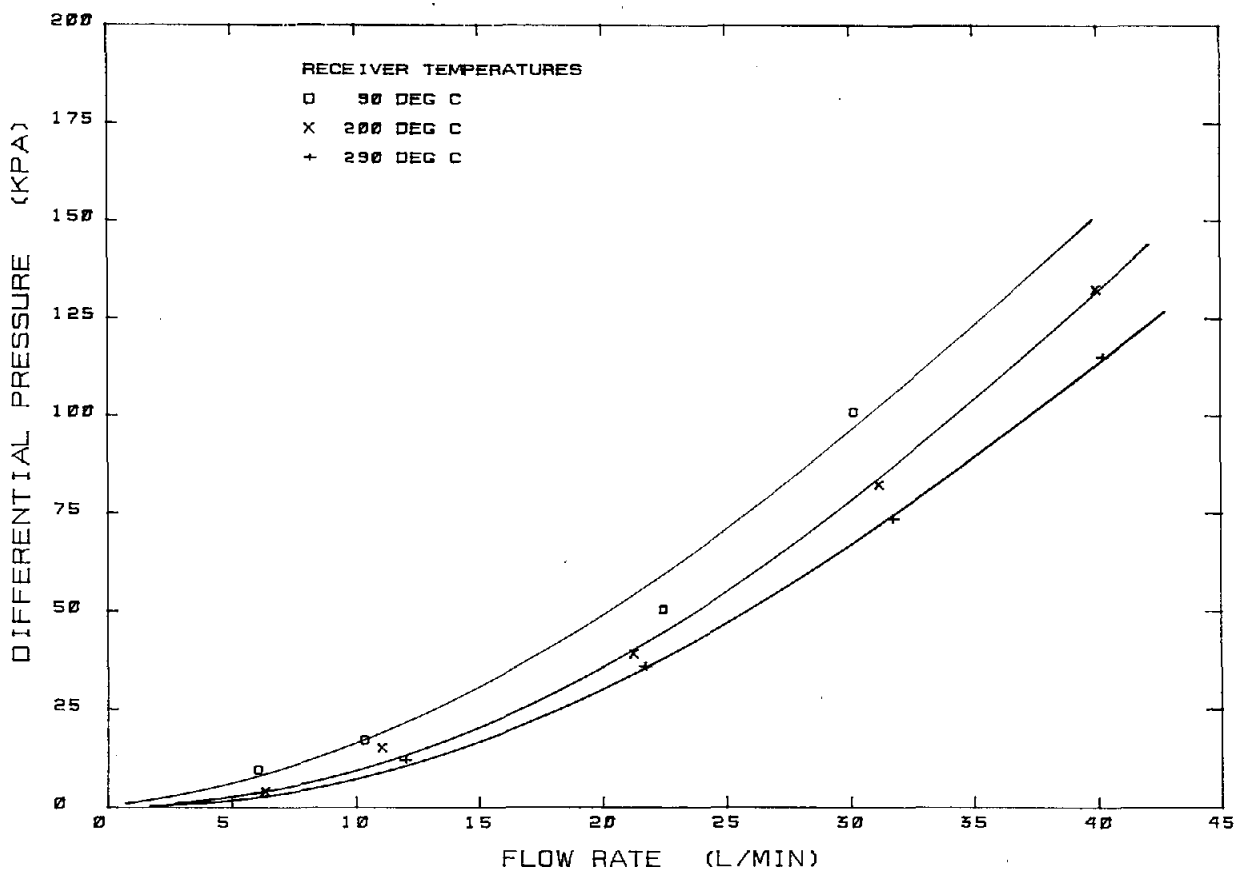

FIGURE 14 SCIENTIFIC ATLANTA RECEIVER DIFFERENTIAL PRESSURE

References

1. Sandia Laboratories, Solar Total Energy Program Plan, SAND76-0167 (Revised).
2. J. L. Russell, Jr., E. P. DePlomb, and R. K. Bansal, Principles of the Fixed Mirror Solar Concentrator, General Atomic Company Report GA-A12902, May 31, 1974.
3. Monsanto Company, Therminol 66, Technical Data Sheet, IC/FF-35.
4. T. Harrison, W. Dworzak, and C. Folkner, Solar Collector Module Test Facility, Instrumentation Fluid Loop Number One, Sandia Laboratories, SAND76-0425, January 1977.

Distribution
TID-4500-R66,UC62(268)

Aerospace Corporation
101 Continental Blvd.
El Segundo, CA 90245
Attn: Elliott L. Katz

Acurex Aerotherm
485 Clyde Avenue
Mountain View, CA 94042
Attn: G. J. Neuner

American Technological Univ.
Solar Total Energy Program
P.O. Box 1416
Killeen, TX 76541
Attn: B. L. Hale

Argonne National Laboratory (3)
9700 South Cass Avenue
Argonne, IL 60439
Attn: R. G. Matlock
W. W. Schertz
Roland Winston

Atlantic Richfield Co.
515 South Flower Street
Los Angeles, CA 90071
Attn: H. R. Blieden

Barber Nichols Engineering
6325 W. 55th Avenue
Arvada, CO 80002
Attn: R. G. Olander

Battelle Memorial Institute
Pacific Northwest Laboratory
P.O. Box 999
Richland, WA 99352
Attn: K. Drumheller

Brookhaven National Laboratory
Associated Universities, Inc.
Upton, LI, NY 11973
Attn: J. Blewett

Centro De Fisica da Materia Condensada
Av. Prof. Gama Pinto, 2
1.699 Lisboa Codex
Portugal
Attn: Manuel Collares Pereira

Congressional Research Service
Library of Congress
Washington, DC 20540
Attn: H. Bullis

Del Manufacturing Co.
905 Monterey Pass Road
Monterey Park, CA 91754
Attn: M. M. Delgado

Desert Research Institute
Energy Systems Laboratory
1500 Buchanan Blvd.
Boulder City, NV 89005
Attn: Jerry O. Bradley

DSET
Black Canyon Stage
P.O. Box 195
Phoenix, AZ 85029
Attn: Gene A. Zerlaut

Honorable Pete V. Domenici
Room 405
Russell Senate Office Bldg.
Washington, DC 20510

Edison Electric Institute
90 Park Avenue
New York, NY 10016
Attn: L.O. Elsaesser

Energy Institute
1700 Las Lomas
Albuquerque, NM 87131
Attn: T. T. Shishman

EPRI
3412 Hillview Avenue
Palo Alto, CA 94303
Attn: J. E. Bigger

General Atomic
P.O. Box 81608
San Diego, CA 92138
Attn: Alan Schwartz

General Electric Company
Valley Forge Space Center
Valley Forge, PA 19087
Attn: Walt Pijawka

General Electric Company
P.O. Box 8661
Philadelphia, PA 19101
Attn: A. J. Poche

Georgia Institute of Technology
School of Mechanical Engineering
Atlanta, GA 30332
Attn: S. Peter Kezios
President
American Society of
Mechanical Engineers

Georgia Institute of Technology
Atlanta, GA 30332
Attn: J. D. Walton

Georgia Power Company
Atlanta, GA 30302
Attn: Mr. Walter Hensley
Vice President
Economics Services

Gruman Corporation
4175 Veterans Memorial Highway
Ronkonkoma, NY 11779
Attn: Ed Diamond

Hexcel
11711 Dublin Blvd.
Dublin, CA 94566
Attn: George P. Branch

Industrial Energy Control Corp
118 Broadway
Hillsdale, NJ 07675
Attn: Peter Groome

Jet Propulsion Laboratory
4800 Oak Grove Drive
Pasadena, CA 91103
Attn: V. C. Truscello

Kingston Industries Corp.
205 Lexington Avenue
New York, NY 10016
Attn: Ken Brandt

Lawrence Berkley Laboratory
University of California
Berkley, CA 94720
Attn: Mike Wallig

Distribution (Cont)

Lawrence Livermore Laboratory
University of California
P.O. Box 808
Livermore, CA 94500
Attn: W. C. Dickinson

Los Alamos Scientific Lab (3)
Los Alamos, NM 87545
Attn: J. D. Balcomb
C. D. Bankston
D. P. Grimmer

Honorable Manuel Lujan
1324 Longworth Building
Washington, DC 20515

Mann-Russell Electronics Inc.
1401 Thorne Roade
Tacoma, WA 98421
Attn: G. R. Russell

Martin Marietta Aerospace
P.O. Box 179
Denver, CO 80201
Attn: R. C. Rozycki

McDonnell Douglas Astronautics Co
5301 Bolsa Avenue
Huntington Beach, CA 92647
Attn: Don Steinmeyer

NASA-Lewis Research Center
Cleveland, OH 44135
Attn: R. Hyland

New Mexico State University
Solar Energy Department
Las Cruses, NM 88001

Oak Ridge Associated Universities
P.O. Box 117
Oak Ridge, TN 37830
Attn: A. Roy

Oak Ridge National Laboratory (4)
P.O. Box Y
Oak Ridge, TN 37830
Attn: J. R. Blevins
C. V. Chester
J. Johnson
S. I. Kaplan

Office of Technology Assessment
U.S. Congress
Washington, DC 20510
Attn: Dr. Henry Kelly

Omnium G (2)
1815 Orangethorpe Park
Anaheim, CA 92801
Attn: Ron Derby
S. P. Lazzara

PRC Energy Analysis Company
7600 Old Springhouse Road
McLean, VA 22102
Attn: K. T. Cherian

Rocket Research Company
York Center
Redmond, WA 98052
Attn: R. J. Stryer

Honorable Harold Runnels
1535 Longworth Building
Washington, DC 20515

Honorable Harrison H. Schmitt
Room 1251
Dirksen Senate Office Bldg.
Washington, DC 20510

Scientific Atlanta, Inc.
3845 Pleasantdale Road
Atlanta, GA 30340
Attn: Andrew L. Blackshaw

Sensor Technology, Inc.
21012 Lassen Street
Chatsworth, CA 91311
Attn: Irwin Rubin

Solar Energy Research Institute (9)
1536 Cole Blvd.
Golden, CO 80401
Attn: C. J. Bishop
Ken Brown
B. L. Butler
D. Kearney
Frank Kreith
R. Gee
B. P. Gupta
A. Rabl
M. Cotton

Solar Energy Technology
Rocketdyne Division
6633 Canoga Avenue
Canoga Park, CA 91304
Attn: J. M. Friefeld

Solar Kinetics, Inc.
P.O. Box 10764
Dallas, TX 75207
Attn: Gus Hutchison

Southwest Research Institute
P.O. Box 28510
San Antonio, TX 78284
Attn: Danny M. Deffenbaugh

Stanford Research Institute
Menol Park, CA 94025
Attn: Arthur J. Slemmons

Stone & Webster
Box 5406
Denver, CO 80217
Attn: V. O. Staub

Sun Gas Company
Suite 800, 2 No. Pk. E.
Dallas, TX 75231
Attn: R. C. Clark

Sundstrand Electric Power
4747 Harrison Avenue
Rockford, IL 61101
Attn: A. W. Adam

Sunsearch, Inc.
669 Boston Post Road,
Guilford, CT 06437
Attn: E. M. Barber, Jr.

Suntec Systems Inc.
2101 Wooddale Dr.
St. Paul, MN 55119
Attn: J. H. Davison

Swedlon, Inc.
12111 Western Avenue
Garden Grove, CA 92645
Attn: E. Nixon

Distribution (Cont)

TEAM Inc.
8136 Ola Keene Mill Road
Springfield, VA 22152

U. S. Department of Energy (2)
Agricultural & Industrial Process Heat
Conservation & Solar Application
Washington, DC 20545
Attn: W. W. Auer
J. Dollard

U. S. Department of Energy (3)
Albuquerque Operations Office
P.O. Box 5400
Albuquerque, NM 87185
Attn: G. Pappas
C. Quinn
J. Weisiger

U. S. Department of Energy
Division of Energy Storage Systems
Washington, DC 20545
Attn: C. J. Swet

U. S. Department of Energy (7)
Division of Central Solar Technology
Washington, DC 20545
Attn: R. H. Annan
G. W. Braun
H. Coleman
M. U. Gutstein
G. M. Kaplan
Lou Melamed
J. E. Rannels

U. S. Department of Energy
Los Angeles Operations Office
350 S. Figueroa Street
Suite 285
Los Angeles, CA 90071
Attn: Fred A. Blaski

U. S. Department of Energy
San Francisco Operations Office
1333 Broadway, Wells Fargo Bldg.
Oakland, CA 94612
Attn: Jack Blasy

University of Delaware
Institute of Energy Conservation
Newark, DE 19711
Attn: K. W. Boer

Watt Engineering Ltd.
RR1, Box 183 1/2
Cedaredge, CO 81413
Attn: A. D. Watt

Western Control Systems
13640 Silver Lake Drive
Poway, CA 92064
Attn: L. P. Cappiello

Westinghouse Electric Corp.
P.O. Box 10864
Pittsburgh, PA 15236
Attn: J. Buggy

1500 W. A. Gardner
1550 F. W. Neilson
2300 J. C. King
3161 J. E. Mitchell
3700 J. C. Strassell
4000 A. Narath
4531 J. H. Renken
4700 J. H. Scott
4710 G. E. Brandvold
4720 V. L. Dugan
4721 J. V. Otts (30)
4722 J. F. Banas
4723 W. P. Schimmel
4725 J. A. Leonard
4730 H. M. Stoller
5512 H. C. Hardee
5520 T. B. Lane
5600 D. B. Shuster
5834 D. M. Mattox
Attn: 5831 N. J. Magnani
5840 H. J. Saxton
Attn: 5810 R. G. Kepler
5820 R. L. Schwoebel
5830 M. J. Davis
5844 F. P. Gerstle
Attn: 5842 J. N. Sweet
5846 E. K. Beauchamp
8100 L. Gutierrez
8450 R. C. Wayne
8266 E. A. Aas
8470 C. S. Selvage
9572 L. G. Rainhart
9700 R. W. Hunnicutt
Attn: 9740 H. H. Pastorius
3141 T. L. Werner (5)
3151 W. L. Garner (3)
For DOE/TIC
(Unlimited Release)